

Emergence of Skyrme crystal in Gross-Neveu and 't Hooft models at finite density

Verena Schön and Michael Thies

*Institute for Theoretical Physics III, University of Erlangen-Nürnberg,
Staudtstr. 7, 91058 Erlangen, Germany*

Abstract

We study two-dimensional, large N field theoretic models (Gross-Neveu model, 't Hooft model) at finite baryon density near the chiral limit. The same mechanism which leads to massless baryons in these models induces a breakdown of translational invariance at any finite density. In the chiral limit baryonic matter is characterized by a spatially varying chiral angle with a wave number depending only on the density. For small bare quark masses a sine-Gordon kink chain is obtained which may be regarded as simplest realization of the Skyrme crystal for nuclear matter. Characteristic differences between confining and non-confining models are pointed out.

1) Introduction

The description of baryonic matter on the basis of QCD remains a theoretical challenge, especially since lattice gauge calculations have so far been of little help for this problem. Nuclear physics, relativistic heavy-ion physics and astrophysics are some of the fields which would greatly benefit from any progress on this issue. Recently, a new surge of interest has been triggered by the suggestion that at high density, the novel phenomenon of color superconductivity might set in [1, 2]. This development has highlighted how little is known reliably about dense, strongly interacting matter.

Here, we address a much simpler finite density problem where a full analytic solution can be found: We consider two-dimensional model field theories with interacting fermions at or near the chiral limit. Specifically, we have in mind the two-dimensional version of the Nambu–Jona-Lasinio model [3], *i.e.*, the chiral Gross-Neveu model [4], and QCD₂ with fundamental quarks, the 't Hooft model [5]. In both cases, one considers a large number N of fermion species and investigates the limit $N \rightarrow \infty$, keeping Ng^2 fixed [6]. These two models are quite similar as far as their chiral properties are concerned but differ with respect to confinement of quarks which is only exhibited by the 't Hooft model. So far, the phase diagram of the Gross-Neveu model has been studied extensively as function of temperature and chemical potential [7, 8, 9, 10, 11], and the results seem to be uncontroversial. The 't Hooft model on the other hand has been investigated only sporadically at finite temperature [20, 21], most recently in Ref. [22], but hardly anything is known yet about its properties at finite density [21].

Our point of departure is the following observation: Both of these models possess light baryons whose mass vanishes in the chiral limit [23, 24, 25] (by light, we mean that M_B/N is small on the relevant physical scale). This is of course no accident, but a generic feature of models with broken chiral symmetry in 1+1 dimension — the baryons are topologically non-trivial excitations of the Goldstone boson (“pion”) field. By contrast, the Gross-Neveu model with discrete chiral symmetry can only accommodate baryons whose mass scales with the physical fermion mass and hence stays finite in the chiral limit. Nevertheless, it has been argued that both variants of the Gross-Neveu model have identical phase diagrams [11]. Since we find it rather perplexing that the structure of the single baryon should have no influence on the structure of baryonic matter, we have reinvestigated this issue. We have found that a combination of large N techniques with the strong constraints arising from broken chiral symmetry is powerful enough to allow for a simple, analytic solution of this problem in the vicinity of the chiral limit. The results of our analysis differ qualitatively from the conventional wisdom about the Gross-Neveu model and carry over to the (confining) 't Hooft model as well. They seem to confirm a number of investigations of other field theories at finite fermion density, where strikingly similar behaviour was found. These include exact studies of two-dimensional models like the massive [12] and massless Schwinger model [13] or finite N_c and N_f massless QCD₂ [14] as well as more approximate treatments of 4-dimensional large N QCD [15, 16, 17] and effective chiral quark models [18, 19].

A word of caution is in order here: Throughout this paper, we shall constantly

deal with spontaneous breaking of continuous symmetries and Goldstone bosons in 1+1 dimensions, in seeming conflict with the Coleman-Mermin-Wagner theorem [26, 27]. It is well understood by now that the large N limit enables one to circumvent this no-go theorem. As clearly explained by Witten [28], the bad infrared behaviour of the boson propagator, when exponentiated, gives rise to a power law correlator $|x - y|^{-1/N}$ which becomes constant in the limit $N \rightarrow \infty$. This kind of almost long-range order is also familiar from the two dimensional XY -model [29, 30]. Alternatively, one may argue that the mean field approximation predicts symmetry breakdown and that this result is protected against fluctuations (which would otherwise restore the symmetry in two dimensions) by $1/N$ suppression factors. In this sense, low dimensional large N theories are not only more tractable, but also physically more appealing than their finite N counterparts. They bear more resemblance to the real, 3+1 dimensional world.

This paper is organized as follows. In Sect. 2 we briefly review the conventional analytical treatment of the chiral Gross-Neveu model at finite density and point out a certain deficiency of this approach. In Sect. 3 we repeat a similar analysis for the 't Hooft model, supplementing the analytical methods by numerical computations where necessary. In Sect. 4 the Skyrme [31] type of approach to the light baryons in both models is recalled [24] and generalized to the case of baryonic matter in the strict chiral limit. In Sect. 5 we then allow for a small symmetry breaking mass term and make contact with the sine-Gordon kink chain, the two dimensional analog of the Skyrme crystal [32]. This is followed by a short summary and conclusions in Sect. 6.

2) Chiral Gross-Neveu model at finite density: Conventional approach

Let us first recall the standard treatment of the Gross-Neveu model at finite density. In the large N limit mean-field techniques become exact. Technically, they may be phrased in a variety of ways. We choose the language of relativistic many-body theory, following Refs. [24, 25, 33], which we find particularly intuitive for the problem at hand. Then the vacuum, the baryon and baryonic matter are all described by a relativistic Hartree-Fock approach (for baryons in the large N limit this was first recognized in Ref. [34]). “Conventional approach” in the title of this section refers to translational invariance — we shall assume that the system is described by an interacting Fermi gas with prescribed, homogeneous density. We shall first deal with the Gross-Neveu model with continuous chiral symmetry ($\psi \rightarrow e^{i\alpha\gamma_5}\psi$) and Lagrangian density [4]

$$\mathcal{L} = \bar{\psi}i\partial\psi + \frac{1}{2}g^2 \left((\bar{\psi}\psi)^2 + (\bar{\psi}i\gamma_5\psi)^2 \right) . \quad (1)$$

As a matter of fact, the corresponding calculation would be identical for the model with discrete chiral symmetry only ($\psi \rightarrow \gamma_5\psi$), where the γ_5 -term in Eq. (1) is omitted. The results presented here are well known, but our aim is to criticize them in a novel way.

We denote the fermion density per color (or baryon density) by $\rho_B = p_f/\pi$ (p_f : Fermi momentum). At the mean field level, the fermions acquire a physical mass m

which has to be determined self-consistently. The ground state energy density per color is given by

$$\frac{\mathcal{E}}{N} = -2 \int_{p_f}^{\Lambda/2} \frac{dk}{2\pi} \sqrt{m^2 + k^2} + \frac{m^2}{2Ng^2} \quad (2)$$

where Λ is an ultra-violet cutoff. The first term is just the sum over single particle energies for all occupied states (the Dirac sea plus all positive energy states with $|p| < p_f$), the second term the usual correction for double counting of interaction effects familiar from the Hartree-Fock approximation. To renormalize the theory, let us first consider the limit $p_f \rightarrow 0$, denoting the physical fermion mass in the vacuum by m_0 ,

$$\frac{\mathcal{E}}{N} = -2 \int_0^{\Lambda/2} \frac{dk}{2\pi} \sqrt{m_0^2 + k^2} + \frac{m_0^2}{2Ng^2} . \quad (3)$$

Minimizing \mathcal{E} with respect to m_0 yields the relativistic Hartree-Fock equation

$$m_0 \left(1 + \frac{Ng^2}{\pi} \ln \frac{m_0}{\Lambda} \right) = 0 . \quad (4)$$

Due to the similarity in structure between the relativistic Hartree-Fock approach and BCS theory [35], this is often referred to as the ‘‘gap equation’’. The non-trivial solution (which has always lower vacuum energy) yields the relation

$$\frac{Ng^2}{\pi} \ln \frac{\Lambda}{m_0} = 1 \quad (5)$$

which teaches us how the bare coupling constant depends on the cutoff parameter, given m_0 . Recall that the Gross-Neveu model shares with real QCD both asymptotic freedom and dimensional transmutation; these properties are contained in Eq. (5). Using this relation to renormalize the matter ground state energy density, Eq. (2), we find (dropping an irrelevant term $-\Lambda^2/8\pi$)

$$\frac{\mathcal{E}}{N} = -\frac{m^2}{4\pi} + \frac{1}{2\pi} p_f \sqrt{p_f^2 + m^2} + \frac{1}{2\pi} m^2 \ln \left(\frac{p_f + \sqrt{m^2 + p_f^2}}{m_0} \right) . \quad (6)$$

The energy is minimal provided m satisfies

$$m \ln \left(\frac{p_f + \sqrt{m^2 + p_f^2}}{m_0} \right) = 0 , \quad (7)$$

i.e., for

$$m = 0 \quad \text{or} \quad m = m_0 \sqrt{1 - \frac{2p_f}{m_0}} \quad \left(p_f < \frac{m_0}{2} \right) . \quad (8)$$

The corresponding energy densities are

$$\begin{aligned} \frac{\mathcal{E}}{N} \Big|_{m=0} &= \frac{p_f^2}{2\pi} , \\ \frac{\mathcal{E}}{N} \Big|_{m \neq 0} &= -\frac{m_0^2}{4\pi} + \frac{p_f m_0}{\pi} - \frac{p_f^2}{2\pi} \quad \left(p_f < \frac{m_0}{2} \right) . \end{aligned} \quad (9)$$

The physical quark masses (8) and the energy densities (9) are plotted in Figs. 1 and 2. From these figures one might be tempted to conclude that chiral symmetry is broken at low densities and gets restored in a second order phase transition at $p_f = m_0/2$. As is well known, this does not occur, rather there is a first order chiral phase transition at $p_f = m_0/\sqrt{2}$. This can easily be inferred by inspection of the thermodynamic potential of the Gross-Neveu model [9]. For our purpose, the following physical reasoning is perhaps more instructive: Let us compare the energy densities (9) with the energy density for a system of size L divided into two homogeneous regions I (size ℓ) and II (size $L - \ell$). In region I chiral symmetry is restored; it contains the extra fermions needed to get the prescribed average density (the ‘‘MIT bag’’ [36]). Region II consists of the physical vacuum with broken chiral symmetry, void of excess fermions. The mean energy density obtained in this way is

$$\frac{\mathcal{E}}{N} = - \left(\frac{L - \ell}{L} \right) \frac{m_0^2}{4\pi} + \frac{L p_f^2}{2\pi \ell} . \quad (10)$$

Minimization with respect to ℓ yields

$$\ell = \frac{\sqrt{2} p_f L}{m_0} \quad (11)$$

valid for $p_f < m_0/\sqrt{2}$, and hence the optimal energy density

$$\frac{\mathcal{E}}{N} = -\frac{m_0^2}{4\pi} + \frac{p_f m_0}{\sqrt{2}\pi} \quad \left(p_f < \frac{m_0}{\sqrt{2}} \right) . \quad (12)$$

As shown in Fig. 2, this solution is lower in energy than the homogeneous one; moreover, it yields the convex hull of \mathcal{E} . It ends exactly at the first order phase transition point $p_f = m_0/\sqrt{2}$ where all space is filled with one big bag. This should be contrasted to the scenario underlying Fig. 1 where the fermion mass decreases continuously. We thus recover the generally accepted mixed phase interpretation of the Gross-Neveu model at finite density. Notice also that only the total size of regions I and II matters, not how they are subdivided; there could be baryon ‘‘droplets’’ as well. Alternatively, the mixed phase curve in Fig. 2 with its linear dependence on p_f could have been inferred from a standard Maxwell construction. It is interesting that a very similar qualitative behaviour was found recently in 3+1 dimensions, where the close relationship with the bag model was also stressed [1].

One important point to which we would like to draw the attention of the reader is the behaviour of \mathcal{E} near $\rho_B = p_f/\pi = 0$. Since ultimately, at very low density, the fermionic matter problem must reduce to the problem of a single baryon, one would expect

$$\left. \frac{\partial \mathcal{E}}{\partial \rho_B} \right|_{\rho_B=0} = M_B \quad (13)$$

where M_B is the baryon mass. In the present calculation, M_B is not the physical baryon mass, but the mass of an alleged ‘‘delocalized’’ baryon. This is inherent in the translationally invariant Hartree-Fock approach, *i.e.*, the assumption that the single particle orbitals are momentum eigenstates. Using Eq. (13) we obtain in the homogeneous, single phase

calculation, Eq. (9), $M_B = Nm_0$, consistent with a short range force and a delocalized baryon. The (physically more viable) mixed phase approach, Eq. (12), predicts a baryon mass lower by a factor of $1/\sqrt{2}$. This factor can readily be understood in terms of the bag model. Indeed, it follows from Eq. (10) that ($E = \mathcal{E}L$)

$$E_B - E_0 = N\ell \left(\frac{m_0^2}{4\pi} + \frac{q_f^2}{2\pi} \right), \quad q_f = \frac{\pi B}{\ell}. \quad (14)$$

For $B = 1$, this expression can be interpreted as energy of a single baryon, ℓ being its diameter. The first term is just the bag pressure (the difference between the energy density of the physical vacuum and that of the perturbative one, cf. Eq. (9) for $p_f = 0$), the second the kinetic energy of N massless quarks. The bag size ℓ is found through minimization of the energy (for $B = 1$) to be

$$\ell = \frac{\sqrt{2}\pi}{m_0}. \quad (15)$$

Inserting this result into Eq. (14), one finds that the bag pressure and the quark kinetic energy contributions are exactly equal in this model and that $M_B = Nm_0/\sqrt{2}$.

However, the Gross-Neveu model possesses bound baryons with lowest mass Nm_0/π (kink solution for the model with discrete chiral symmetry [4, 33]), or even massless baryons (model with continuous chiral symmetry [24]). These binding effects are not $1/N$ suppressed and should be correctly reproduced in a Hartree-Fock approach, in the low density limit. They have obviously been missed here due to our tacit assumption of translational invariance. There is no good reason why such effects should not play a role at higher densities as well. Moreover, differences between the continuous and discrete chirally symmetric Gross-Neveu models based on their different baryon structure and masses are not at all captured by the ‘‘conventional’’ approach. Below, we shall present a cure for this disease. Before that however, let us first repeat the naive calculation for the ’t Hooft model, where the corresponding results are not yet available in the literature.

3) ’t Hooft model at finite density, assuming translational invariance

The ’t Hooft model is defined as the large N limit of 1+1 dimensional $SU(N)$ gauge theory with quarks in the fundamental representation [5],

$$\mathcal{L} = \bar{\psi}i\not{D}\psi - \frac{1}{2}\text{tr}F_{\mu\nu}F^{\mu\nu}. \quad (16)$$

Since the light-cone approach originally used by ’t Hooft to determine the meson spectrum seems to be less convenient for the vacuum, baryon and baryonic matter problems, we shall work in normal coordinates. This approach was pioneered by Bars and Green [37] and further developed in Refs. [38, 24, 25]. Common to all of these works is the fact that the gluons are gauged away (axial gauge), leaving behind a theory of fermions interacting

via a linear Coulomb potential. We refer the reader to the detailed derivation of the Hartree-Fock approach in Refs. [24, 25] and immediately proceed to the formulae which are relevant for our purpose. Let us first summarize the treatment of the vacuum. A central quantity is the single particle density matrix in momentum space,

$$\rho(p) = \frac{1}{2} + \gamma^0 \rho_0(p) - i\gamma^1 \rho_1(p) + \gamma^5 \rho_5(p) . \quad (17)$$

Its precise definition in terms of the quark fields is

$$\rho_{\alpha\beta}(p) = \int dx e^{-ipx} \langle 0 | \frac{1}{N} \sum_i \psi_{i\beta}^\dagger(0) \psi_{i\alpha}(x) | 0 \rangle . \quad (18)$$

The Slater determinant condition characteristic for Hartree-Fock,

$$\rho^2(p) = \rho(p) \rightarrow \rho_0^2(p) + \rho_1^2(p) + \rho_5^2(p) = 1/4 \quad (19)$$

holds manifestly in the parametrization

$$\begin{pmatrix} \rho_0(p) \\ \rho_1(p) \\ \rho_5(p) \end{pmatrix} = -\frac{1}{2} \begin{pmatrix} \sin \theta(p) \cos \varphi \\ \sin \theta(p) \sin \varphi \\ \cos \theta(p) \end{pmatrix} . \quad (20)$$

$\theta(p)$ is the Bogoliubov angle, φ the global angle which locates the broken symmetry vacuum on the chiral circle (hence it has no p -dependence). The Bogoliubov angles are the variational parameters; this terminology stems once more from BCS theory, which has the same formal structure as relativistic Hartree-Fock. We choose $\varphi = 0$, the value reached if one lets the bare quark mass approach zero starting from a finite value. Then,

$$\rho(p) = v(p) v^\dagger(p) \quad (21)$$

with the (positive and negative energy) Hartree-Fock spinors

$$u(p) = \begin{pmatrix} \cos \theta(p)/2 \\ \sin \theta(p)/2 \end{pmatrix} , \quad v(p) = \begin{pmatrix} -\sin \theta(p)/2 \\ \cos \theta(p)/2 \end{pmatrix} . \quad (22)$$

The vacuum expectation value of the Hamiltonian density reads

$$\frac{\mathcal{E}}{N} = - \int \frac{dp}{2\pi} p \cos \theta(p) - \frac{Ng^2}{8} \int \frac{dp}{2\pi} \int \frac{dp'}{2\pi} \frac{\cos(\theta(p) - \theta(p')) - 1}{(p - p')^2} \quad (23)$$

where the first term is the kinetic energy, the second the Coulomb interaction of the quarks. Varying with respect to the Bogoliubov angles $\theta(p)$, the gap equation is obtained in the form

$$p \sin \theta(p) + \frac{Ng^2}{4} \int \frac{dp'}{2\pi} \frac{\sin(\theta(p) - \theta(p'))}{(p - p')^2} = 0 . \quad (24)$$

The integral has to be defined as principal value integral, cf. Refs. [37, 38, 25]. We shall also need the expression for the quark condensate in the vacuum,

$$\langle \bar{\psi} \psi \rangle_v = -N \int \frac{dp}{2\pi} \sin \theta(p) , \quad (25)$$

and the quark single particle energies,

$$\omega(p) = p \cos \theta(p) + \frac{Ng^2}{4} \int \frac{dp' \cos(\theta(p) - \theta(p'))}{2\pi (p - p')^2}. \quad (26)$$

Although the gap equation (24) for the 't Hooft model must be solved numerically, the value of the quark condensate (25) is known analytically, owing to an indirect determination via sum rules and the 't Hooft equation for mesons [39]; it is

$$\langle \bar{\psi}\psi \rangle_v = -\frac{N}{\sqrt{12}} \left(\frac{Ng^2}{2\pi} \right)^{1/2}. \quad (27)$$

The single particle energies (26) are badly infrared divergent, a source of a long and ongoing debate in the literature [40]. To exhibit the divergence, we follow Ref. [25], isolate the divergent part of the integral and regularize it by using a finite box of length L ,

$$\omega(p) = p \cos \theta(p) + \frac{Ng^2}{4} \int \frac{dp' \cos(\theta(p) - \theta(p')) - 1}{2\pi (p - p')^2} + \frac{Ng^2 L}{48}. \quad (28)$$

This last constant diverges for $L \rightarrow \infty$ but seems to be essential to account for confinement in such an independent particle picture: The isolated quarks behave roughly as if they had infinite mass. If one simply throws the infinite constant away, as is often done, one gets an awkward sign change in $\omega(p)$ at some low momentum p , cf. Refs. [38, 24, 25], and runs into serious inconsistencies in finite temperature Hartree-Fock calculations [21, 22]. Fortunately, the constant drops out of the calculation of color singlet mesons, as already noticed by 't Hooft (his IR cutoff parameter λ is related to our box size L by $\lambda = 12/\pi L$, cf. Ref. [25]): The infinite self-energy term is cancelled by an equally infinite piece in the Coulomb interaction. We also note in passing that if one employs a finite box as infrared regulator, one is unambiguously led to 't Hooft's treatment of the quark self-energies rather than to Wu's alternative regularization prescription [41, 40]. Since the emergence of the constant $Ng^2 L/48$ in the single particle energy (28), but not in the vacuum energy (23), is rather important for our discussion and somewhat hidden in Ref. [25], we have included a simplified version of the arguments underlying Eqs. (23) and (28) in the appendix.

After this review of the treatment of the vacuum, we are in a position to include a finite baryon density, assuming translational invariance. If p_f denotes the Fermi momentum, we have to replace the density matrix (21) by

$$\begin{aligned} \rho(p) &= \Theta(p_f - |p|)u(p)u^\dagger(p) + v(p)v^\dagger(p) \\ &= \Theta(p_f - |p|) + \Theta(|p| - p_f)v(p)v^\dagger(p) \end{aligned} \quad (29)$$

where we have used the completeness relation for the spinors in the second step. In the expression for the Hartree-Fock ground state energy density (23), according to the second line of Eq. (29), we must exclude the region $[-p_f, p_f]$ from the momentum integrations and pick up an additional term due to the change in the baryon density $\text{tr}\rho$,

$$\frac{\mathcal{E}}{N} = - \int \frac{dp}{2\pi} \Theta(|p| - p_f) p \cos \theta(p)$$

$$\begin{aligned}
& -\frac{Ng^2}{8} \int \frac{dp}{2\pi} \int \frac{dp'}{2\pi} \Theta(|p| - p_f) \Theta(|p'| - p_f) \frac{\cos(\theta(p) - \theta(p')) - 1}{(p - p')^2} \\
& + \frac{Ng^2}{4} \int \frac{dp}{2\pi} \int \frac{dp'}{2\pi} \Theta(p_f - |p|) \Theta(|p'| - p_f) \frac{1}{(p - p')^2} .
\end{aligned} \tag{30}$$

This yields at once the following finite density generalization of the gap equation,

$$p \sin \theta(p) + \frac{Ng^2}{4} \int \frac{dp'}{2\pi} \Theta(|p'| - p_f) \frac{\sin(\theta(p) - \theta(p'))}{(p - p')^2} = 0 , \quad (|p| > p_f) , \tag{31}$$

whereas the condensate now becomes

$$\langle \bar{\psi} \psi \rangle = -N \int \frac{dp}{2\pi} \theta(|p| - p_f) \sin \theta(p) . \tag{32}$$

The gap equation (31) can easily be solved numerically for various p_f . The resulting condensate is shown in Fig. 3. We find that it decreases monotonically with increasing density, disappearing at a critical Fermi momentum

$$p_f^c \approx 0.117 \left(\frac{Ng^2}{2\pi} \right)^{1/2} . \tag{33}$$

This behaviour is strikingly similar to the corresponding result for the Gross-Neveu model depicted in Fig. 1, again suggesting some phase transition with restoration of chiral symmetry at high density. Here we are not able to go on and discuss whether we are dealing with a first or second order phase transition. The reason lies in the following problem: If we compute the energy density (30) for the 't Hooft model we discover that subtraction of the value at $p_f = 0$ is not sufficient to give a finite result. Unlike in the Gross-Neveu model, the difference is still IR divergent. To be able to proceed, we enclose the system once more in a box of length L . We then find that the divergence is due to the last term in Eq. (30) (the one which does not involve the Bogoliubov angles) which now contributes the following double sum to the energy per color,

$$\frac{E}{N} \Big|_{\text{div}} = \frac{Ng^2 L}{16\pi^2} \sum_{p \in I} \sum_{n \neq 0, (p-n) \notin I} \frac{1}{n^2} . \tag{34}$$

Here antiperiodic boundary conditions for fermions have been employed in the box regularization, and correspondingly the interval I is defined in the following way,

$$I = [-n_f, n_f] \quad \text{for } B = 2n_f + 1 \text{ odd} , \quad I = [-n_f - 1, n_f] \quad \text{for } B = 2n_f + 2 \text{ even} . \tag{35}$$

The result (34) is even more alarming than the non-convex behaviour of \mathcal{E} in the Gross-Neveu model, Fig. 2, due to its L -dependence. Adding quarks to the vacuum causes the energy to increase by an infinite amount in the limit $L \rightarrow \infty$. Evaluating the double sums in Eq. (34) for low values of B , we obtain information on the origin of this divergent behaviour. For $B = 1$ ($I = [0, 0]$) in particular, the calculated baryon mass (to leading order in L) is

$$M_B = N \left(\frac{Ng^2 L}{48} \right) . \tag{36}$$

This is the same relation as $M_B = Nm_0$ in the Gross-Neveu model except that the physical fermion mass is replaced by the infinite constant $Ng^2L/48$ characteristic of confinement, cf. Eq. (28). For larger values of B Eq. (34) does not simply yield multiples of the baryon mass (36), but one finds “interaction effects” of the same order of magnitude as the mass. As far as N -counting is concerned, this is still in agreement with Witten’s analysis of baryons at large N [34]. However, since these delocalized baryons are presumably not very physical in the ’t Hooft model, we refrain from further discussing these effects.

Summarizing, the problems encountered in the Gross-Neveu model with translationally invariant baryonic matter again show up in the ’t Hooft model, although in a much more severe form. The physics reason is clear: In the Gross-Neveu model the cost of distributing N fermions over the whole space is governed by their physical mass; in the ’t Hooft model, due to confinement of quarks, the corresponding quark effective mass diverges with the volume. On the other hand, it is known that both models do possess massless, delocalized baryons in the chiral limit. Evidently, this has to be accounted for, and we conclude that the naive, translationally invariant Hartree-Fock approximation fails miserably in describing the properties of baryonic matter.

4) Massless baryons and baryonic matter in the Skyrme picture

The existence of massless baryons in the chiral limit of the ’t Hooft model has been demonstrated by bosonization [23, 40], variational [24], and light-cone [25] techniques. These exotic objects are characteristic for 1+1 dimensional models with broken chiral symmetry and, as such, also present in the chiral Gross-Neveu model. A particularly illuminating derivation is due to Salcedo *et al.* [24]. These authors point out that the potential energy in such models is invariant under local chiral transformations, unlike the kinetic term which is only invariant under global ones. This led them to the following variational ansatz for the one-body density matrix of the baryon,

$$\rho(x, y) = e^{i\chi(x)\gamma_5} \rho_v(x - y) e^{-i\chi(y)\gamma_5} . \quad (37)$$

Here $\rho_v(x - y)$ is the vacuum density matrix. If the vacuum breaks chiral symmetry, one can generate with expression (37) a new (exact or approximate) Hartree-Fock solution which breaks translational invariance but can carry non-zero baryon number. As shown in [24], the baryon density is given by

$$\rho_B(x) = \text{tr}(\rho(x, x) - \rho_v(0)) = \frac{1}{\pi} \partial_x \chi(x) , \quad (38)$$

so that the baryon number coincides with the winding number of the chiral phase $\chi(x)$,

$$B = \int_0^L dx \frac{1}{\pi} \partial_x \chi = \frac{\chi(L) - \chi(0)}{\pi} \in \mathbb{Z} . \quad (39)$$

(Notice that $\chi(L) - \chi(0)$ must be an integer multiple of π since otherwise bilinear fermion observables would no longer be periodic.) For this topological reasoning it is again recommendable to work in a finite box of size L . The topological interpretation of the baryon

number also agrees with exact results of Ref. [25] which were not restricted to the large N limit. In the absence of an explicit quark mass term, the ground state energy obtained from Eq. (37) is

$$E[\rho] = E[\rho_v] + N \int_0^L dx \frac{1}{2\pi} (\partial_x \chi)^2 . \quad (40)$$

This result holds independently of the specific model, since the potential energy does not contribute to $E[\rho] - E[\rho_v]$. Differences between various models are of course still present in the vacuum density matrix ρ_v in Eq. (37) but do not manifest themselves in the baryon energy. Minimizing $E[\rho]$ with respect to χ yields the free (static) bosonic equation

$$\partial_x^2 \chi(x) = 0 , \quad \chi(L) = \chi(0) + \pi B \quad (41)$$

with the solution

$$\chi(x) = \pi B \left(\frac{x - x_0}{L} \right) . \quad (42)$$

Here x_0 is a parameter which reflects the breakdown of translational invariance. The baryon density is x -independent ($\rho_B(x) = B/L$) as follows more generally from axial current conservation in the chiral limit [24]. However, the scalar and pseudoscalar condensates acquire a non-trivial x -dependence,

$$\begin{aligned} \langle \bar{\psi} \psi \rangle &= \langle \bar{\psi} \psi \rangle_v \cos(2\pi B(x - x_0)/L) , \\ \langle \bar{\psi} i\gamma_5 \psi \rangle &= -\langle \bar{\psi} \psi \rangle_v \sin(2\pi B(x - x_0)/L) . \end{aligned} \quad (43)$$

Since fluctuations of $\chi(x)$ describe the massless Goldstone boson field, the baryon picture emerging here is very similar in spirit to the Skyrme model [31]. The fact that the baryon is a topological soliton will become somewhat clearer once we include a small bare quark mass (see Sect. 5) but this solitonic character also holds in the strict chiral limit considered here.

We can now discuss the baryon as well as baryonic matter from this point of view. The single baryon ($B = 1$) is spread out over the whole space, the chiral phase $\chi(x)$ making one turn with constant speed to minimize the kinetic energy (Fig. 4). The baryon energy is, using Eqs. (40-42),

$$E_B = N \frac{\pi}{2L} . \quad (44)$$

This confirms that indeed the baryon becomes massless in the limit $L \rightarrow \infty$. Incidentally, expression (44) is identical to the kinetic energy of N non-interacting, massless quarks in the lowest momentum state available for antiperiodic boundary conditions. Nevertheless, we are not dealing with the free, chirally symmetric theory, but with the broken phase of an interacting theory where the quarks are massive or even confined.

It may be worthwhile to contemplate the structure of the baryon for a moment from the point of view of the relativistic Hartree-Fock approximation. In chirally non-invariant models one would suspect that the baryon comprises the filled Dirac sea plus one filled, positive energy valence level. This is exactly what one finds analytically in the non-chiral Gross-Neveu model [33], or numerically in QCD₂ with heavy quarks [24]. The picture implied by the ansatz (37) in the chiral limit is rather different though. Denoting

the negative energy single particle orbitals in the Dirac sea by $\varphi_k^{(-)}(x)$ (solutions of the first quantized Dirac equation with Hartree-Fock potential), the Skyrme type baryon (37) admits the density matrix

$$\rho(x, y) = e^{i\pi x\gamma_5/L} \sum_k \varphi_k^{(-)}(x) \varphi_k^{(-)\dagger}(y) e^{-i\pi y\gamma_5/L} \quad (45)$$

where

$$\varphi_k^{(-)}(x) = e^{ikx} v(k) , \quad (46)$$

and the k are discrete momenta appropriate to the interval of length L . We first observe that the chiral phase factor splits the momenta of the right- and left-handed components into $k \pm \pi/L$. Since the transformed single particle wave functions are no longer momentum eigenstates, translational invariance is lost. Secondly, we note that the presence of an infinite Dirac sea is crucial for getting the extra baryon charge, rather than a single valence state. If the sum over occupied states k in Eq. (45) was finite, we would trivially conclude that $\rho(x, y)$ and $\rho_v(x - y)$ belong to the same baryon density ($\rho_B(x) = \text{tr}\rho(x, x)$). Due to the infinite number of occupied states however, $\rho_v(x - y)$ develops a singularity at $x = y$, and one has to do a more careful point splitting in order to compute the baryon density. The divergence is due to the UV region and therefore determined by the free theory (for more details, cf. Ref. [24]),

$$\lim_{x \rightarrow y} \text{tr}(\rho(x, y) - \rho_v(x - y)) = \lim_{z \rightarrow 0} \text{tr} \left\{ e^{i\pi z\gamma_5/L} \left(\frac{1}{2}\delta(z) - \frac{i\gamma_5}{2\pi z} \right) - \frac{1}{2}\delta(z) \right\} = \frac{1}{L} . \quad (47)$$

The result $1/L$ is the baryon density for $B = 1$. This mechanism is strongly reminiscent of the calculation of anomalous current commutators, for instance in the Schwinger model. The extra baryon number does not reside in a valence level added on top of the Dirac sea but somehow emerges from the bottom of the Dirac sea if one modifies all the levels slightly — it is a vacuum polarization effect.

Equipped with this exotic kind of baryon, we can now easily find the ground state of the system for any baryon density. As discussed above and illustrated in Fig. 4, the single baryon consists of one turn of a “chiral spiral” (parametrized by $\chi(x)$) over the total spatial length L of the system — admittedly a somewhat elusive object in the thermodynamic limit. A finite density $\rho_B = B/L = p_f/\pi$ on the other hand implies that

$$\chi(x) = p_f(x - x_0) , \quad (48)$$

i.e., one full rotation over a physical distance which has a well defined limit for $L \rightarrow \infty$, namely $2/\rho_B$. The baryon density remains constant in space, but the condensates are modulated as

$$\begin{aligned} \langle \bar{\psi}\psi \rangle &= \langle \bar{\psi}\psi \rangle_v \cos 2p_f(x - x_0) , \\ \langle \bar{\psi}i\gamma_5\psi \rangle &= -\langle \bar{\psi}\psi \rangle_v \sin 2p_f(x - x_0) . \end{aligned} \quad (49)$$

They can be viewed as projections of a “chiral spiral” of radius $|\langle \bar{\psi}\psi \rangle_v|$ onto two orthogonal planes, see Fig. 5. This state breaks translational symmetry; it is a crystal. In fact, it may be viewed as the simplest possible realization of the old idea of a Skyrme crystal [32],

here in the context of large N two-dimensional field theories. One cannot tell where one baryon begins and ends — each full turn of the spiral contains baryon number 1. Only the condensates reveal that translational symmetry has been broken down to a discrete subgroup. The energy density of this unusual kind of “nuclear matter” is simply (after subtracting the vacuum energy density)

$$\frac{\mathcal{E}}{N} = \frac{p_f^2}{2\pi}. \quad (50)$$

Surprisingly, this is exactly what one would expect for a free Fermi gas of massless quarks although Eq. (50) holds for interacting theories where the vacuum has lower energy due to chiral symmetry breaking. In Fig. 6 we compare the energy density for this state to the ones discussed above for the Gross-Neveu model, where translational symmetry had been assumed. The crystal is always energetically favored, the dependence on p_f is now convex, and there is no trace of a phase transition, neither first nor second order, at any density. The horizontal slope at $p_f = 0$ correctly signals the presence of massless baryons and eliminates the above mentioned problems with the spurious massive, delocalized baryons. We cannot even draw the corresponding picture for the ’t Hooft model, simply because in this case the quark Fermi gas is infinitely higher in energy than the Skyrme crystal for $L \rightarrow \infty$. Nevertheless, all the results for baryonic matter discussed in this section apply to the ’t Hooft model as well.

In the high density limit the oscillations of the condensates become more and more rapid. If we are interested only in length scales large as compared to $1/p_f$, the condensates average to zero. In this sense, one might argue that chiral symmetry gets restored at high density, although not in the naive way suggested by Fig. 2.

Finally, we remark that the “chiral spiral” ground state for fixed baryon density still preserves one continuous, unbroken symmetry, namely the combination of translation and chiral rotation generated by $P + p_f Q_5$ (P : momentum operator, Q_5 : axial charge). One would therefore predict that RPA excitations on this ground state [24, 25] (or mesons in nuclear matter) will have only one collective, gapless mode, a hybrid of a “phonon” and a “pion”.

5) Non-vanishing bare quark masses

In Ref. [24] the Skyrme picture of the baryons in the ’t Hooft model and chiral Gross-Neveu model was developed for small, finite bare quark masses, using the expression in Eq. (37) as a variational ansatz. For a single baryon, these authors have tested the accuracy of their procedure against the full, numerical Hartree-Fock calculation on a lattice. The results agreed perfectly at $m_q = 0.05$ and were still surprisingly good at $m_q = 0.20$, in units of $\sqrt{Ng^2/2\pi}$. This makes it very tempting to speculate that the corresponding variational calculation can also give us a reliable picture of baryonic matter at finite density, away from the chiral limit. As compared to the formulae in the preceding section, the only change is the fact that the bare mass term now also contributes to the energy functional

Eq. (40),

$$E[\rho] = E[\rho_v] + N \int_0^L dx \left\{ \frac{1}{2\pi} (\partial_x \chi)^2 + \frac{m_q \langle \bar{\psi} \psi \rangle_v}{N} (\cos 2\chi - 1) \right\} . \quad (51)$$

Here the condensate $\langle \bar{\psi} \psi \rangle_v$ refers to the vacuum in the chiral limit. Varying with respect to $\chi(x)$ then gives the static sine-Gordon equation [42],

$$\partial_x^2 \chi + \frac{2\pi m_q \langle \bar{\psi} \psi \rangle_v}{N} \sin 2\chi = 0 , \quad (52)$$

from which one reads off the ‘‘pion’’ mass (two dimensional version of the Gell Mann-Oakes-Renner relation [43])

$$m_\pi^2 = -4\pi m_q \frac{\langle \bar{\psi} \psi \rangle_v}{N} . \quad (53)$$

The $B = 1$ baryon can be identified with the familiar kink solution of the sine-Gordon equation,

$$\chi(x) = 2 \arctan \left(e^{m_\pi(x-x_0)} \right) , \quad (54)$$

with mass

$$M_B = N \frac{2m_\pi}{\pi} . \quad (55)$$

Since the single baryon has been discussed in detail in Ref. [24], let us immediately turn to multi-kink solutions as candidates for baryonic matter. Luckily, the sine-Gordon kink crystal has already been studied thoroughly in the literature, first in solid state physics [44, 45] and more recently as a toy model for the Skyrme crystal [46], in terms of Jacobi elliptic functions and elliptic integrals [47]. We take over the results from Ref. [46] which is close in spirit to the present study although the authors did not have in mind two-dimensional large N field theories. Adapting the formulae of this work to our notation, the following steps allow us to generalize the Skyrme crystal of the previous section to small, finite bare quark masses: Let m_π denote the mass of the Goldstone boson, Eq. (53), and $\bar{\rho}_B = p_f/\pi$ the average baryon density (this is our definition of p_f for the case of broken translational symmetry). We then first have to solve the transcendental equation

$$\frac{\pi m_\pi}{p_f} = 2k \mathbf{K}(k) \quad (56)$$

for k where $\mathbf{K}(k)$ is the complete elliptic integral of the first kind. The sine-Gordon kink crystal is then given by the following solution of Eq. (52),

$$\chi(x) = \frac{\pi}{2} + \text{am}(\xi, k) , \quad \xi = \frac{m_\pi}{k}(x - x_0) , \quad (57)$$

($\text{am}(\xi, k)$ is the Jacobian elliptic amplitude function). From this, we can express the baryon density and the various condensates in terms of further Jacobian elliptic functions (dn , sn , cn) as follows,

$$\begin{aligned} \rho_B(x) &= \frac{1}{\pi} \partial_x \chi(x) = \frac{m_\pi}{\pi k} \text{dn}(\xi, k) , \\ \langle \bar{\psi} \psi \rangle &= \langle \bar{\psi} \psi \rangle_v \cos 2\chi(x) = -\langle \bar{\psi} \psi \rangle_v \left(\text{cn}^2(\xi, k) - \text{sn}^2(\xi, k) \right) , \\ \langle \bar{\psi} i\gamma_5 \psi \rangle &= -\langle \bar{\psi} \psi \rangle_v \sin 2\chi(x) = \langle \bar{\psi} \psi \rangle_v 2\text{sn}(\xi, k) \text{cn}(\xi, k) . \end{aligned} \quad (58)$$

Here ξ is as defined in Eq. (57). Finally, the energy divided by the volume of this kind of matter is given by

$$\frac{\mathcal{E}}{N} = \frac{m_\pi p_f}{4\pi^2} \left\{ \frac{8}{k} \mathbf{E}(k) + 4k \left(1 - \frac{1}{k^2} \right) \mathbf{K}(k) \right\} , \quad (59)$$

$\mathbf{E}(k)$ denoting the complete elliptic integral of the second kind.

Let us now illustrate these results in two regimes of interest, namely at low and high density. At low density ($p_f \ll m_\pi$) k in Eq. (56) approaches 1 exponentially, and the baryon density features a chain of well resolved lumps whose shape is determined by the single kink solution (Fig. 7). Likewise, the condensates behave like those of a single baryon: $\langle \bar{\psi} \psi \rangle$ changes from the vacuum value outside the baryons to its negative in their center whereas $\langle \bar{\psi} i \gamma_5 \psi \rangle$ is peaked in the surface region of each baryon (Figs. 8, 9). These condensates are projections of the distorted ‘‘chiral spiral’’ shown in Fig. 10. The energy (59) for low densities behaves as

$$\mathcal{E} \approx N \frac{2m_\pi p_f}{\pi^2} = M_B \rho_B , \quad (60)$$

showing the expected connection to the baryon mass. At high densities ($p_f \gg m_\pi$), k approaches 0 like

$$k \approx \frac{m_\pi}{p_f} . \quad (61)$$

Thus ξ in Eq. (57) becomes $p_f(x - x_0)$. Moreover, for $k \rightarrow 0$, the Jacobian elliptic functions $\text{am}(\xi, k)$, $\text{sn}(\xi, k)$, $\text{cn}(\xi, k)$ are known to reduce to the argument ξ and the ordinary trigonometric functions $\sin \xi$ and $\cos \xi$, respectively. We thus recover the results for the simple chiral spiral in Sect. 4 (the parameter x_0 has to be readjusted to take care of the shift by $\pi/2$ in Eq. (57)). The energy in this case is approximately

$$\frac{\mathcal{E}}{N} \approx \frac{p_f^2}{2\pi} + \frac{m_\pi^2}{8\pi} . \quad (62)$$

The condensates look very much like the sin- and cos-functions of the massless case and need not be plotted. The baryon density wiggles around a constant value, reflecting the strong overlap of the baryons, and can be approximated at high density by

$$\rho_B(x) \approx \frac{p_f}{\pi} \left(1 - \frac{1}{2} \left(\frac{m_\pi}{p_f} \right)^2 \sin^2 p_f(x - x_0) \right) . \quad (63)$$

The behaviour of the baryon density $\rho_B(x)$ as one increases p_f (*i.e.*, the mean density) is illustrated in Fig. 11. In the chiral- or high-density limit ($m_\pi/p_f \rightarrow 0$) $\rho_B(x)$ eventually becomes x -independent. This provides us with another way of understanding the structure of matter described in the previous section, namely as arising from a chain of very extended, strongly overlapping lumps.

Finally, let us come back to the question of validity of the variational calculation based on the chirally modulated vacuum density matrix (37), which we have left open so far. At very low densities when the individual baryons are far apart, we can presumably

rely on the numerical results of Ref. [24] since the interaction effects between the baryons become small (as discussed in Refs. [24] and [46], the baryon-baryon interaction is repulsive and falls off exponentially with the pion Compton wavelength). At high densities, on the other hand, one would expect that a finite quark mass cannot make much difference as long as $p_f \gg m_\pi$. This takes us back to the massless case discussed in Sect. 4. In this limit, in turn, it is easy to convince oneself that the calculation becomes exact in the sense that one gets a true solution of the Hartree-Fock equation. Thus for instance for the 't Hooft model, the massless Hartree-Fock equation reads [24]

$$\omega_n \varphi_\alpha^{(n)}(x) = -i(\gamma_5)_{\alpha\beta} \frac{\partial}{\partial x} \varphi_\beta^{(n)}(x) + \frac{Ng^2}{4} \int dy |x-y| \rho_{\alpha\beta}(x,y) \varphi_\beta^{(n)}(y). \quad (64)$$

Upon substituting

$$\varphi_\alpha^{(n)}(x) = \left(e^{-ip_f x \gamma_5} \right)_{\alpha\beta} \tilde{\varphi}_\beta^{(n)}(x) \quad (65)$$

as we are instructed to do by the ansatz (37), we discover that $\tilde{\varphi}^{(n)}$ does indeed solve the Hartree-Fock equation, the only change being that the single particle energy ω_n gets replaced by $\omega_n + p_f$. The same argument goes through in the chiral Gross-Neveu model, or in any field theory where the interaction term has a local chiral invariance. This proves that the result becomes exact in the chiral limit (to leading order in the $1/N$ expansion, of course) and makes plausible the hypothesis that it also correctly describes the high density regime for finite quark masses as long as $p_f \gg m_\pi$.

6) Summary and conclusions

In this paper, we have addressed the problem of baryonic matter in a certain class of exactly soluble field theoretic models, namely chirally invariant, large N , interacting fermion theories. We started out from a seemingly innocuous and well understood problem, the chiral Gross-Neveu model at finite density and identified one remaining weak spot: The energy density for baryonic matter in the standard Hartree-Fock approach does not have the correct low density limit which can be predicted from the known baryon spectrum of the theory. The origin of this problem which is not cured by a mixed phase approach conceptionally related to the bag model, is evidently the assumption of translational invariance. Whereas this inconsistency can perhaps be ignored in the Gross-Neveu model (as it has been so far, to the best of our knowledge), in QCD₂, it becomes fatal: Due to confinement, the analogous calculation yields an infinite energy for delocalized baryons or quark matter. This is unavoidable if one is careful in treating the infrared behaviour of the quark single particle energies. These findings have prompted us to think more thoroughly about the structure of baryons in such models and possible implications for the matter problem. We found that it takes only very little effort to generalize a previous Skyrme type treatment of the single, massless baryon to the case of baryonic matter. In the chiral limit, an extremely simple, yet non-trivial, picture emerges: Both the baryon and dense matter are described by a spatially varying chiral angle which is best characterized as a ‘‘chiral spiral’’ with constant helix angle. The number of windings within the full space of length L measures the number of baryons in the box. Since, by construction,

this kind of state does not cost any potential energy in addition to what is already stored in the vacuum, one does not have to pay the expected high price for delocalizing quarks. The energy density of baryonic matter is identical to that of a free Fermi gas of massless quarks, in spite of the presence of interaction effects. The same picture applies to the chiral Gross-Neveu as well as to the massless 't Hooft model and should be generic for all chiral large N models. The baryon density is constant in space as a consequence of axial current conservation, and we have verified that the whole scenario is exact to leading order in the $1/N$ expansion. In a slightly more speculative vein we then investigated modifications due to a small bare quark mass. Here our task was greatly facilitated by the fact that we only needed to pull together two independent investigations, the one of Ref. [24] of the single baryon in field theoretic models with the one of Ref. [46] of the sine-Gordon kink crystal, both inspired in some way by Skyrme's original ideas. As a result, we have arrived at a rather comprehensive picture of matter at low and high density on the scale of the pion Compton wavelength. The crystal structure now becomes more conspicuous since also the baryon density displays a lattice of individual lumps. As an additional bonus, we have obtained a purely classical, mechanical model of what is going on (the sine-Gordon equation describes a chain of coupled pendulums, the quark mass playing the role of gravity). Given our starting point, namely the problem of baryonic matter in two dimensional quantum field theories like the Nambu–Jona-Lasinio model or QCD, this is rather amusing.

It is noteworthy that a similar chiral structure of fermionic matter has been reported previously in a variety of models different from the present ones. This indicates that the basic results are more generally valid than our derivation might suggest. We mention here in particular the early work on the massive Schwinger model [12] and the more recent work on the massless Schwinger model with inert background charge [13] and QCD₂ with a finite number of colors and flavours [14]. Even more surprising are perhaps quite a number of speculations about spatially inhomogeneous chiral condensates with the same wave number as in our case, but in 3+1 dimensions, in the context of pion condensation [18], large N QCD [15, 16, 17], or effective chiral models [19]. In some of these works, the analogy with the Overhauser effect and spin-density waves (pairing of particle holes on opposite sides of the Fermi sphere) has been stressed. Although the language used is quite different from ours, there is no doubt that we are dealing with the same physical phenomenon.

As a last remark, we wish to comment on the original Gross-Neveu model with only discrete chiral symmetry (pure $(\bar{\psi}\psi)^2$ -interaction). Most of the studies of the phase diagram for the Gross-Neveu model have in fact been performed for this model, and one might think that our analysis does not have anything to say about it. However, the criticism of Sect. 2 also applies here. Since the non-chiral Gross-Neveu model has (massive) bound baryons, the low density behaviour of the energy obtained in standard Hartree-Fock approximation cannot be correct, and the phase diagram may also have to be reconsidered.

We thank A.C. Kalloniatis for a critical reading of the manuscript. Partial sup-

port of this work by the Bundesministerium für Bildung, Wissenschaft, Forschung und Technologie is gratefully acknowledged.

Appendix: Hartree-Fock single particle energies in the 't Hooft model

The Hamiltonian for the massless 't Hooft model in the axial gauge has the form

$$H = \sum_{p,i} \frac{2\pi}{L} (p + 1/2) \left(a_i^\dagger(p) a_i(p) - b_i^\dagger(p) b_i(p) \right) + \frac{g^2 L}{16\pi^2} \sum_{ij,n \neq 0} \frac{j_{ij}(n) j_{ji}(-n)}{n^2} . \quad (66)$$

Here we have regularized the theory by enclosing it in a box of length L with antiperiodic boundary conditions for the fermions. Note that this form is only valid in the limit $L \rightarrow \infty$ [22]. The $a_i(p), b_i(p)$ denote right- and left-handed quark operators, respectively, and the currents $j_{ij}(n)$ can be taken in the $U(N)$ form at large N ,

$$j_{ij}(n) = \sum_p \left(a_j^\dagger(p) a_i(p+n) + b_j^\dagger(p) b_i(p+n) \right) . \quad (67)$$

It is important to understand that the Coulomb term still contains one- and two-body operators which can be disentangled by normal-ordering (up to $1/N$ corrections) as follows,

$$\begin{aligned} \sum_{ij} j_{ij}(n) j_{ji}(-n) &= N \sum_{i,p} \left(a_i^\dagger(p) a_i(p) + b_i^\dagger(p) b_i(p) \right) \\ &- \sum_{ij,pq} \left(a_j^\dagger(p) a_j(q) a_i^\dagger(q+n) a_i(p+n) + a_j^\dagger(p) b_j(q) b_i^\dagger(q+n) a_i(p+n) \right. \\ &\quad \left. + b_j^\dagger(p) a_j(q) a_i^\dagger(q+n) b_i(p+n) + b_j^\dagger(p) b_j(q) b_i^\dagger(q+n) b_i(p+n) \right) \end{aligned} \quad (68)$$

The Hamiltonian can be decomposed correspondingly into one- and two-body operators. Using the basic vacuum expectation values

$$\begin{aligned} \sum_i \langle 0 | a_i^\dagger(p) a_i(q) | 0 \rangle &= \frac{N}{2} \delta_{pq} (1 - \cos \theta(p)) , \\ \sum_i \langle 0 | b_i^\dagger(p) b_i(q) | 0 \rangle &= \frac{N}{2} \delta_{pq} (1 + \cos \theta(p)) , \\ \sum_i \langle 0 | a_i^\dagger(p) b_i(q) | 0 \rangle &= \sum_i \langle 0 | b_i^\dagger(p) a_i(q) | 0 \rangle = -\frac{N}{2} \delta_{pq} \sin \theta(p) , \end{aligned} \quad (69)$$

the vacuum expectation value of these two contributions are found to be

$$\begin{aligned} \langle 0 | H^{(1)} | 0 \rangle &= N \sum_p \left(-\frac{2\pi}{L} \left(p + \frac{1}{2} \right) \cos \theta(p) + \frac{Ng^2 L}{48} \right) , \\ \langle 0 | H^{(2)} | 0 \rangle &= N \sum_p \left(-\frac{Ng^2 L}{32\pi^2} \sum_{n \neq 0} \frac{1}{n^2} [1 + \cos(\theta(p) - \theta(p+n))] \right) . \end{aligned} \quad (70)$$

The $Ng^2L/48$ term in the 1-body part is just minus twice the “1” term in the 2-body part (remember that $\sum_{n \neq 0} 1/n^2 = \pi^2/3$). Hence, in the sum of both terms, the Coulomb energy involves the combination

$$\frac{1}{n^2}[\cos(\theta(p) - \theta(p+n)) - 1] \quad (71)$$

where the infrared divergence has been tamed since denominator and numerator both vanish at $n = 0$. This cancellation between quark self-energy and Coulomb potential is similar to what happens in the meson equation of the 't Hooft model. The continuum limit then yields Eq. (23). It is important to distinguish between one- and two-body operators here, because they enter with different relative weights in the single particle energies and in the total energy. Indeed, in the Hartree-Fock approach, if the single particle energies are decomposed according to their 1- and 2-body contributions as

$$\omega(p) = \omega^{(1)}(p) + \omega^{(2)}(p) , \quad (72)$$

then the ground state energy is

$$\langle 0|H|0\rangle = N \sum_p \left(\omega^{(1)}(p) + \frac{1}{2}\omega^{(2)}(p) \right) . \quad (73)$$

The factor 1/2 is necessary to avoid double counting of the 2-body interaction term. By comparison with Eq. (70), we can turn this observation around and simply read off the single particle energies. We find in this way

$$\begin{aligned} \omega^{(1)}(p) &= -\frac{2\pi}{L} \left(p + \frac{1}{2} \right) \cos \theta(p) + \frac{Ng^2L}{48} , \\ \omega^{(2)}(p) &= -\frac{Ng^2L}{16\pi^2} \sum_{n \neq 0} \frac{1}{n^2} (1 + \cos(\theta(p) - \theta(p+n))) . \end{aligned} \quad (74)$$

Adding up the two contributions to $\omega(p)$, the “1” term is now cancelled instead of changing sign. This is the reason why in the continuum limit we get the badly infrared divergent expression (26) for the quark energies. This short-cut derivation gives the same result as the more elaborate approach of Ref. [25], where a single particle Hartree-Fock Hamiltonian was first identified by commuting H with the quark operators and subsequently diagonalized.

References

- [1] M. Alford, K. Rajagopal, and F. Wilczek, Phys. Lett. **B422** (1998) 247.
- [2] R. Rapp, T. Schäfer, E.V. Shuryak, and M. Velkovsky, Phys. Rev. Lett. **81** (1998) 247.
- [3] Y. Nambu and G. Jona-Lasinio, Phys. Rev. **122** (1961) 345.

- [4] D.J. Gross and A. Neveu, Phys. Rev. **D10** (1974) 3235.
- [5] G. 't Hooft, Nucl. Phys. **B75** (1974) 461.
- [6] G. 't Hooft, Nucl. Phys. **B72** (1974) 461.
- [7] B.J. Harrington and A. Yildiz, Phys. Rev. **D11** (1975) 779.
- [8] R.F. Dashen, S. Ma, and R. Rajaraman, Phys. Rev. **D11** (1975) 1499.
- [9] U. Wolff, Phys. Lett. **B157** (1985) 303.
- [10] T.F. Treml, Phys. Rev. **D39** (1988) 679.
- [11] A. Barducci, R. Casalbuoni, M. Modugno, G. Pettini, and R. Gatto, Phys. Rev. **D51** (1995) 3042.
- [12] W. Fischler, J. Kogut, and L.Susskind, Phys. Rev. **D19** (1979) 1188.
- [13] Y-Ch. Kao and Y-W. Lee, Phys. Rev. **D50** (1994) 1165.
- [14] H.R. Christiansen and F.A. Schaposnik, Phys. Rev. **D55** (1997) 4920.
- [15] D.V. Deryagin, D.Yu. Grigoriev, and V.A. Rubakov, Int. J. Mod. Phys. **A7** (1992) 659.
- [16] E. Shuster and D.T. Son, Nucl. Phys. **B573** (2000) 434.
- [17] B-Y. Park, M. Rho, A. Wirzba, and I. Zahed, hep-ph/9910347.
- [18] M. Kutschera, W. Broniowski, and A. Kotlorz, Nucl. Phys. **A516** (1990) 566.
- [19] M. Sadzikowski and W. Broniowski, hep-ph/0003282.
- [20] L.D. McLerran and A. Sen, Phys. Rev. **D32** (1985) 2794.
- [21] Ming Li, Phys. Rev. **D34** (1986) 3888.
- [22] V. Schön and M. Thies, Phys. Lett. **B481** (2000) 299.
- [23] I. Affleck, Nucl. Phys. **B265** (1986) 448.
- [24] L.L. Salcedo, S. Levit, and J.W. Negele, Nucl. Phys. **B361** (1991) 585.
- [25] F. Lenz, M. Thies, S. Levit, and K. Yazaki, Ann. Phys. **208** (1991) 1.
- [26] S. Coleman, Comm. Math. Phys. **31** (1973) 259.
- [27] N.D. Mermin and H. Wagner, Phys. Rev. Lett. **17** (1966) 1133.
- [28] E. Witten, Nucl. Phys. **B145** (1978) 110.
- [29] V.L. Berezinski, Sov. Phys. JETP **32** (1971) 493.

- [30] J.M. Kosterlitz and D. Thouless, J. Phys. **C6** (1973) 1181.
- [31] T.H.R. Skyrme, Proc. Roy. Soc. Lond. **A260** (1961) 127.
- [32] I. Klebanov, Nucl. Phys. **B262** (1985) 133.
- [33] R. Pausch, M. Thies, and V.L. Dolman, Z. Phys. **A338** (1991) 441.
- [34] E. Witten, Nucl. Phys. **B160** (1979) 57.
- [35] J. Bardeen, L.N. Cooper, and J.R. Schrieffer, Phys. Rev. Lett. **34** (1975) 1353.
- [36] A. Chodos, R.L. Jaffe, K. Johnson, C.B. Thorn, and V.F. Weisskopf, Phys. Rev. **D9** (1974) 3471.
- [37] I. Bars and M.B. Green, Phys. Rev. **D17** (1978) 537.
- [38] Ming Li, L. Wilets, and M.C. Birse, J. Phys. **G13** (1987) 915.
- [39] A.R. Zhitnitsky, Phys. Lett. **B165** (1985) 405.
- [40] E. Abdalla and M.C.B. Abdalla, Phys. Rep. **265** (1996) 253.
- [41] T.T. Wu, Phys. Lett. **B71** (1977) 142.
- [42] A.C.Scott, F.Y.F. Chu, and D.W. McLaughlin, Proc. IEEE **61** (1973) 1443.
- [43] M. Gell-Mann, R.J. Oakes, and B. Renner, Phys. Rev. **175** (1968) 2195.
- [44] W.L. McMillan, Phys. Rev. **B16** (1977) 4655.
- [45] G. Theodorou and T.M. Rice, Phys. Rev. **B18** (1978) 2840.
- [46] K. Takayama and M. Oka, Nucl. Phys. **A551** (1993) 637.
- [47] *Handbook of Mathematical Functions*, M. Abramovitz and I.A. Stegun, eds. (Dover, New York, 1970)

Figure captions

1. Physical fermion mass as a function of the Fermi momentum in the Gross-Neveu model, in units of m_0 .
2. Energy density per color as a function of the Fermi momentum in the Gross-Neveu model. Solid curve: Chirally symmetric solution ($m = 0$); diamonds: Broken chiral symmetry (m according to Fig. 1); dashed straight line: Mixed phase. Units of m_0 .
3. Quark condensate as a function of the Fermi momentum in the 't Hooft model, in units of $(Ng^2/2\pi)^{1/2}$.
4. The complex condensate $\langle \bar{\psi}\psi \rangle + i\langle \bar{\psi}i\gamma_5\psi \rangle$ for the single baryon in units of $\langle \bar{\psi}\psi \rangle_v$, as a function of x in units of L (chiral limit).
5. Same as Fig. 4, but for baryonic matter. Each full turn of the spiral increases the baryon number by one unit.
6. Same as Fig. 2 (Gross-Neveu model). Here we have included the energy density of the Skyrme crystal type of state (crosses), the true ground state.
7. Solid curve: Spatial oscillation of the baryon density in the regime $p_f \ll m_\pi$; circles: Baryon density for a single baryon.
8. Solid curve: Spatial oscillations of the scalar chiral condensate in the regime $p_f \ll m_\pi$; circles: Scalar chiral condensate for a single baryon.
9. Same as Fig. 8, but for the pseudoscalar chiral condensate.
10. Illustration of the distorted “chiral spiral” for baryonic matter at non-zero bare quark mass.
11. Spatial dependence of baryon density as it evolves with increasing average density (or Fermi momentum), in units of m_π .

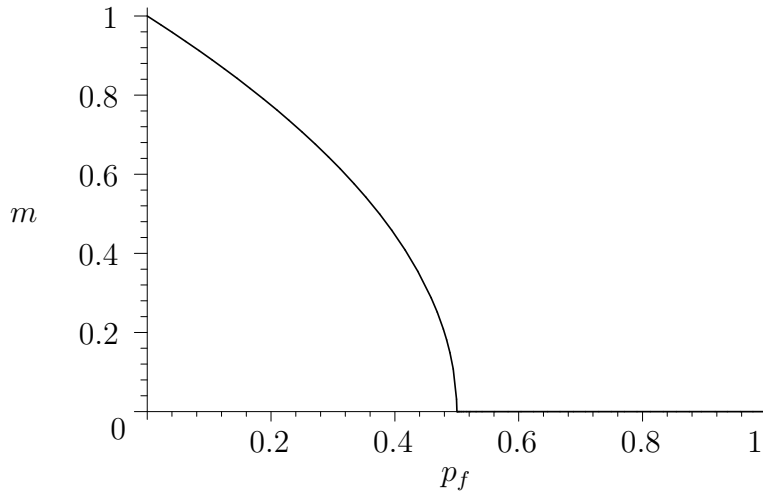


Figure 1

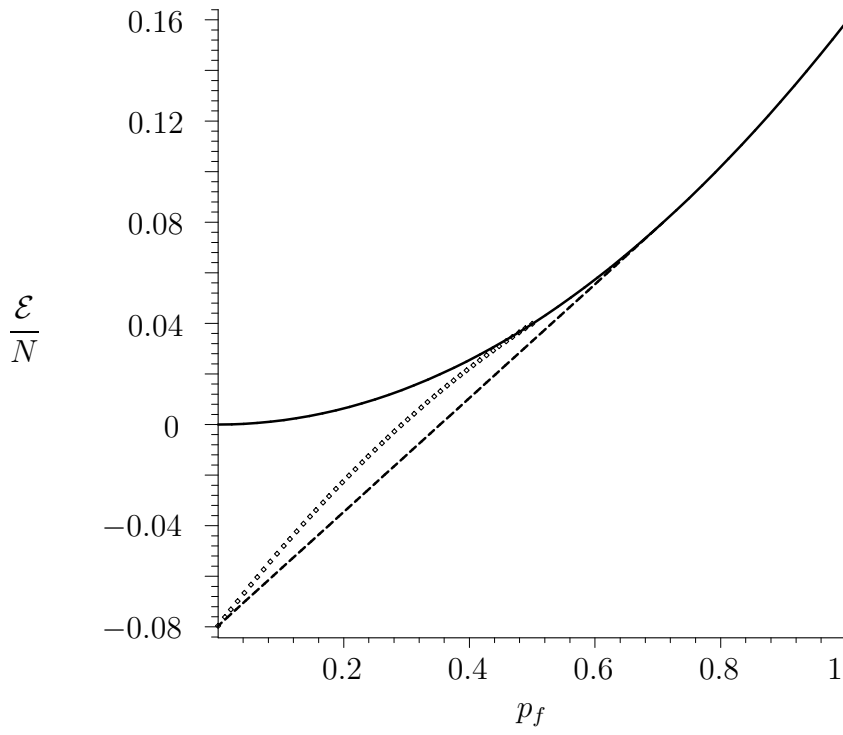


Figure 2

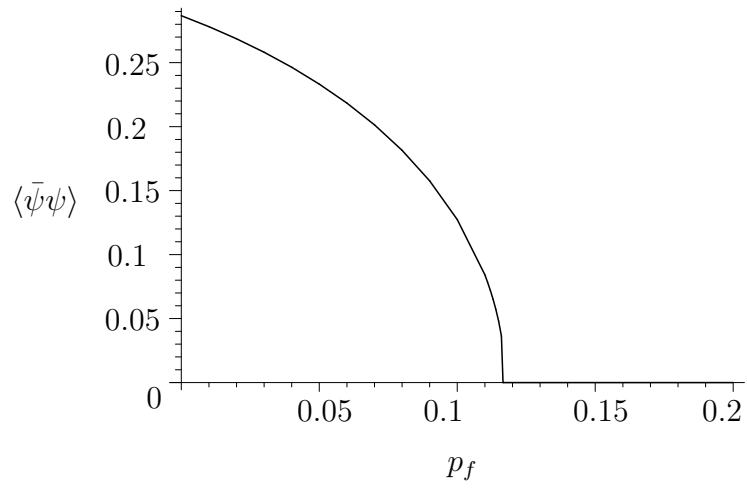


Figure 3

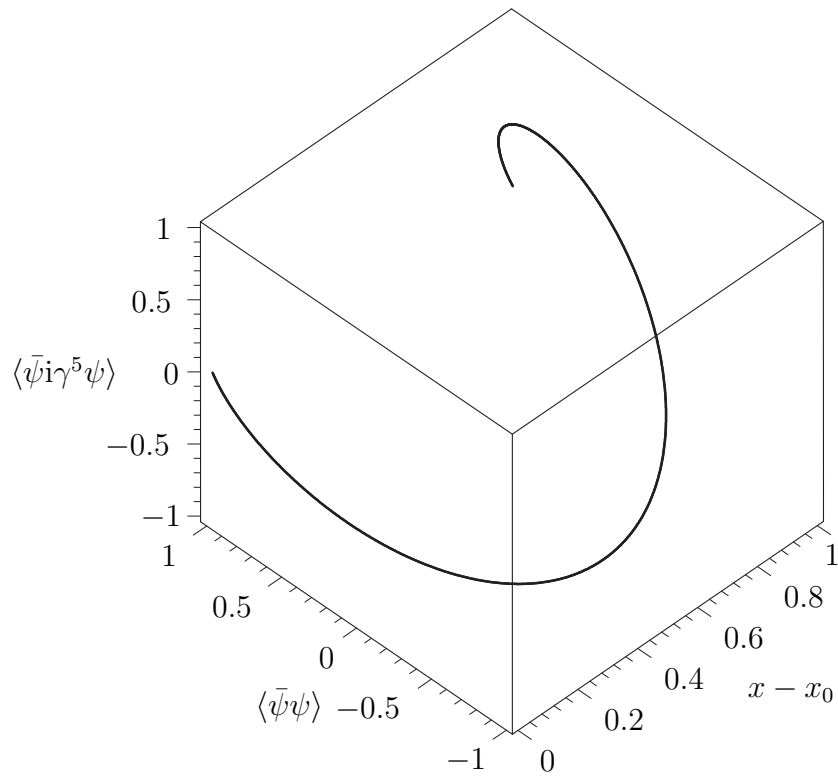


Figure 4

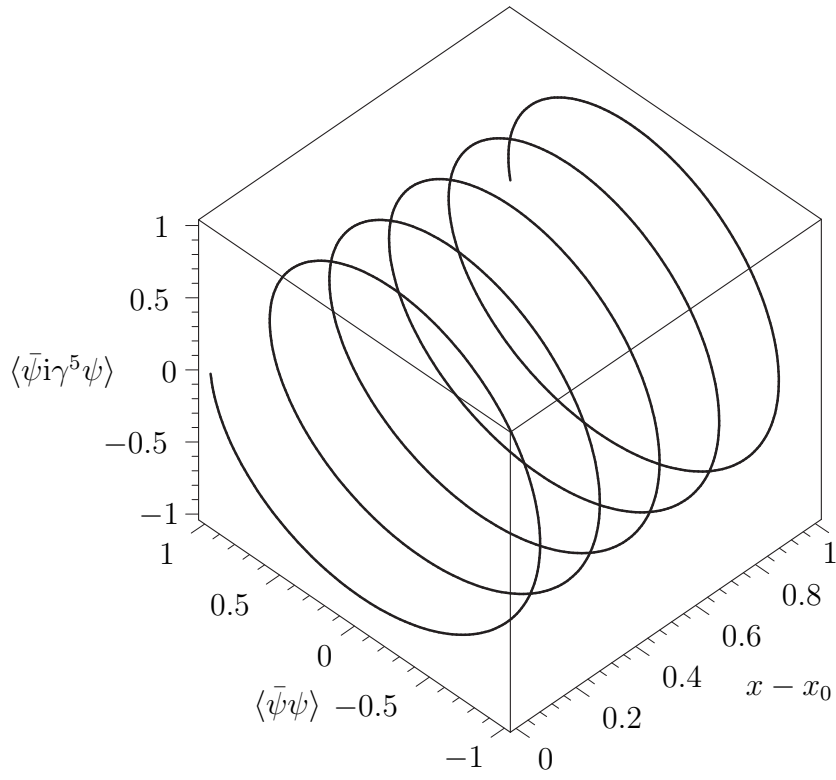


Figure 5

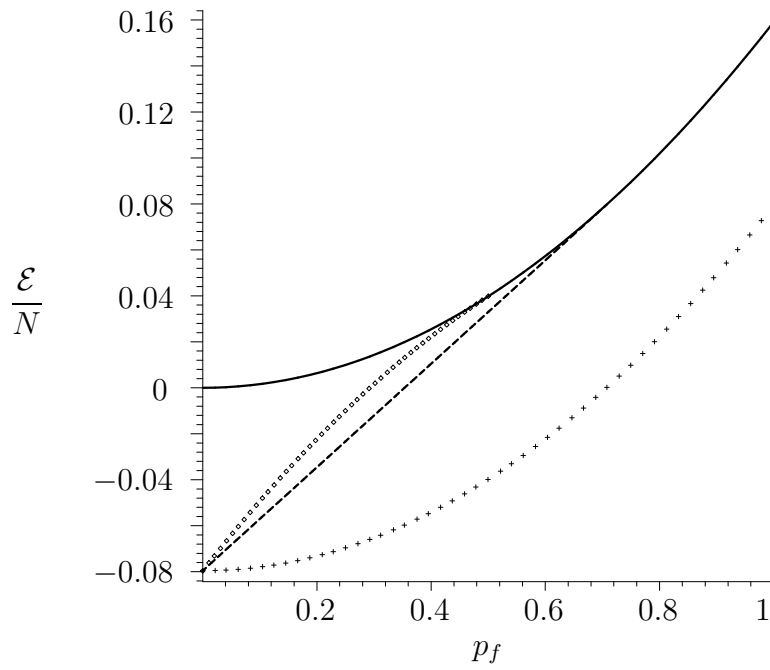


Figure 6

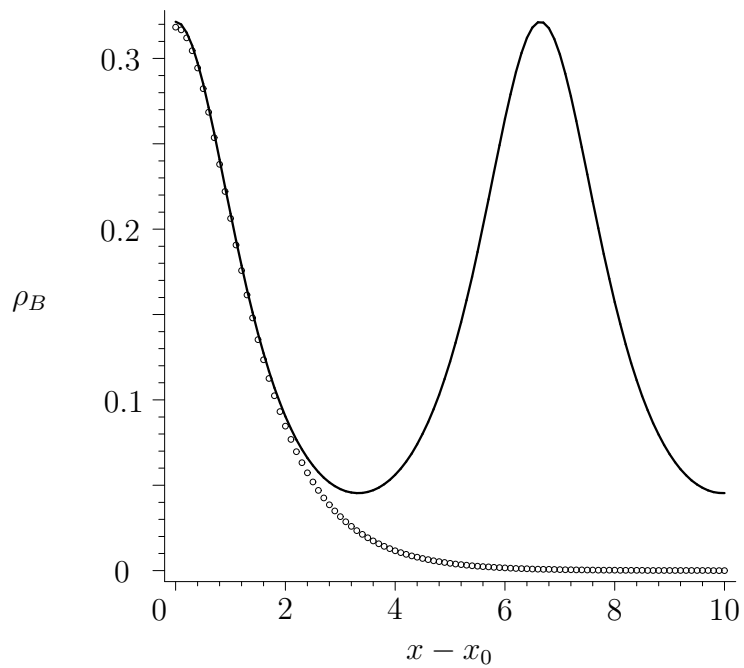


Figure 7

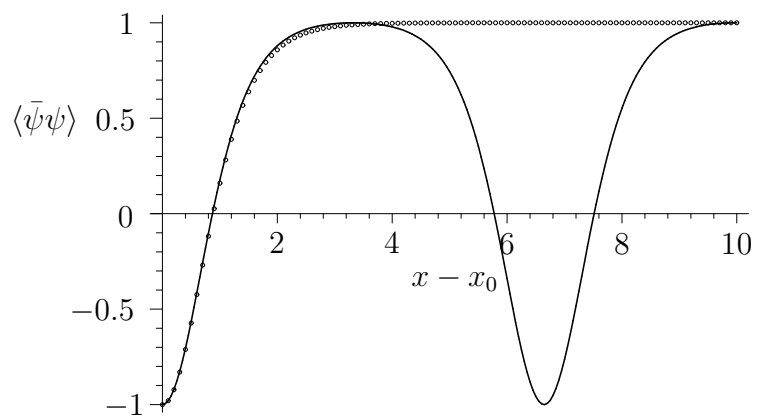


Figure 8

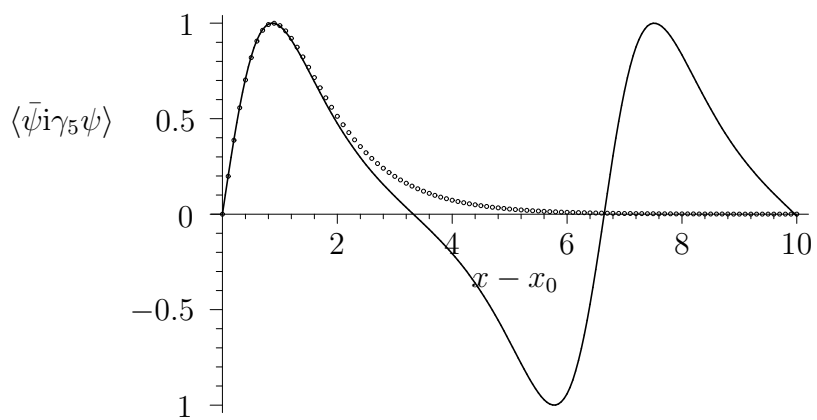


Figure 9

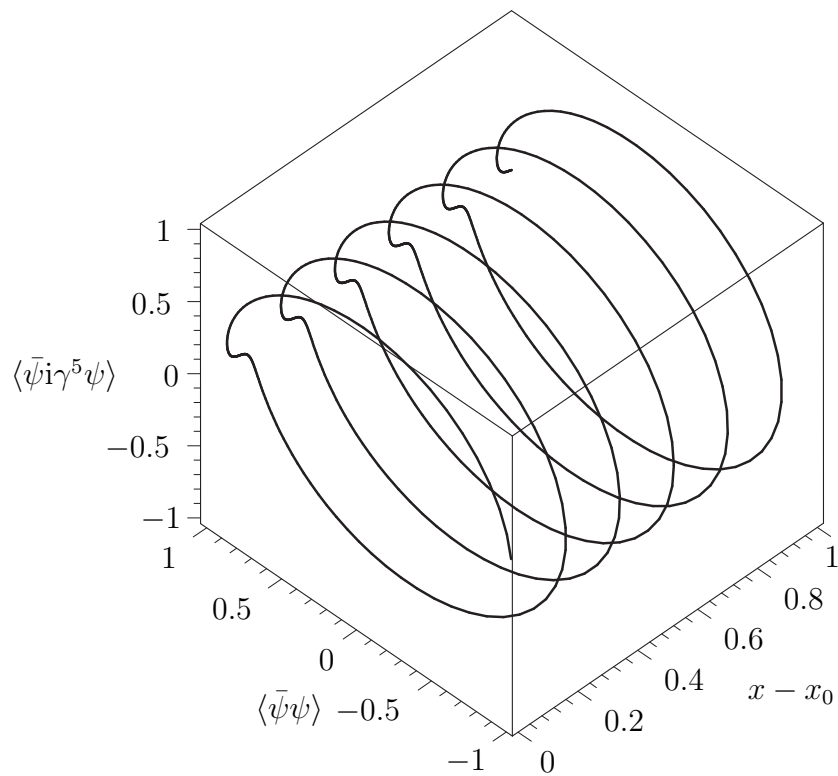


Figure 10

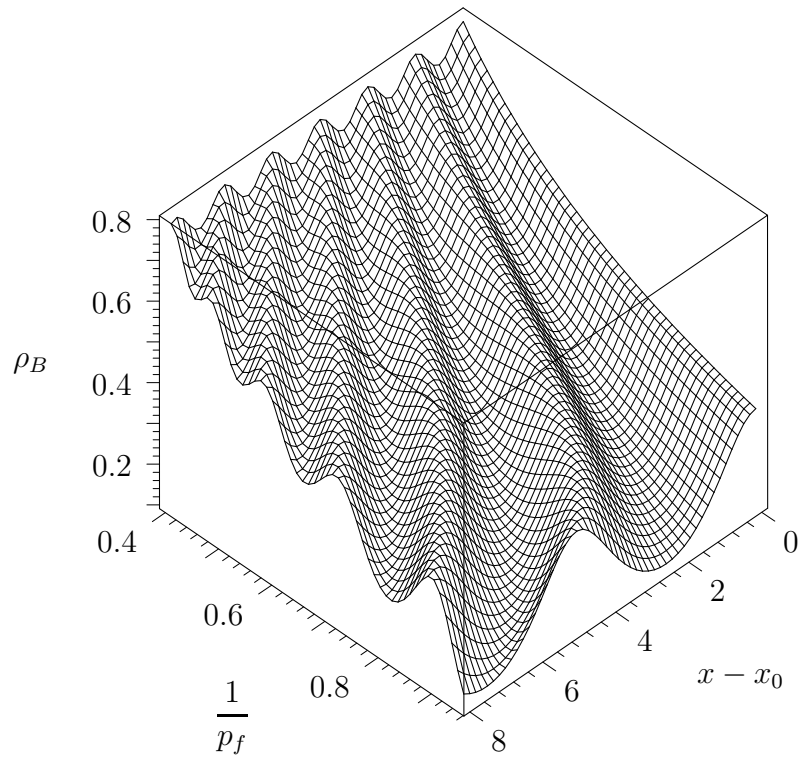


Figure 11